ADVANCES IN ATMOSPHERIC SCIENCES, VOL. 22, NO. 5, 2005, 685–702

Diurnal Variation of Tropical Convection during TOGA COARE IOP

Jae-Young BYON* and Gyu-Ho LIM

School of Earth and Environmental Sciences, Seoul National University, Seoul, South Korea

(Received 18 October 2004; revised 13 June 2005)

ABSTRACT

Diurnal variation of tropical convection and kinematic and thermodynamic conditions was investigated for different large-scale environments of the convectively active and inactive periods by using satellite observations and surface measurements during the Intensive Observation Period (IOP) of the Tropical Ocean Global Atmosphere/Coupled Ocean-Atmosphere Response Experiment (TOGA/COARE). During the convectively active period, the features of nocturnal convection appear in vertical profiles of convergence, vertical velocity, heat source, and moisture sink. The specific humidity increases remarkably in the middle troposphere at dawn. On the other hand, the altitude of maximum convergence and that of the upward motion is lower during the convectively inactive period. The specific humidity peaks in the lower troposphere in the daytime and decreases in the middle troposphere. Spectral analyses of the time series of the infrared (IR) brightness temperature (TBB) and amounts of rainfall suggest multiscale temporal variation with a prominent diurnal cycle over land and oceanic regions such as the Intensive Flux Array (IFA) and the South Pacific Convergence Zone (SPCZ). Over land, the daily maximum of deep convection associated with cloud top temperature less than 208 K appears at midnight due to the daytime radiative heating and the sea-land breeze. Over the ocean, convection usually tends to occur at dawn for the convectively active period while in the afternoon during the inactive period. Comparing the diurnal variation of convection with large-scale variables, the authors inferred that moisture in the middle troposphere contributes mostly to the development of nocturnal convection over the ocean during the convectively active period.

Key words: diurnal variation, tropical convection, rainfall, large-scale environment

1. Introduction

Tropical convection plays an important role in the general circulation and the climate of the Earth by releasing latent heat associated with a phase change of water vapor. The heat released from the tropical convection and precipitation drives the large scale circulations such as the Walker circulation and the Madden-Julian oscillation (MJO). The tropical convection also influences the Earth's radiation budget via interaction with the emission and incidence of solar energy (Hendon and Woodberry, 1993). Hence, study of the temporal variation of tropical convection is essential for understanding the atmospheric circulation.

The temporal variation of tropical convection has been investigated by many authors. It is reported that tropical convection possesses variability with timescales ranging from several hours to many years (Nakazawa, 1988; Sui and Lau, 1992; Weng and Lau, 1994). Among many components of variations with a different period, the diurnal variation is most prominent. Gray and Jacobson (1977) found an early morning maximum in the small islands, while an afternoon maximum in the large islands, based on rain gauge observations in the western Pacific Ocean region. For the tropical Atlantic Ocean, McGarry and Reed (1978) showed that a maximization of convection occurred in the afternoon and at midnight from analysis of Global Atmospheric Research Program Atlantic Tropical Experiment (GATE) observations.

The rain rate retrieved from satellite observation is used for the study of the global diurnal variation of rainfall. Augustine (1984) found a strong afternoon and early morning maximum in the tropical Pacific for August 1979 by analyzing rainfalls retrieved from the SMS-2 IR (infrared) imagery. Chang et al.

*E-mail: byonjy2@snu.ac.kr

(1995) found that the early morning rainfall was larger than the afternoon's, based on the rain rate retrieved from the Special Sensor Microwave/Imager (SSM/I). Imaoka and Spencer (2000) and Nesbitt and Zipser (2003) examined the rainfall derived by the Tropical Rainfall Measuring Mission (TRMM) TMI (TRMM Microwave Imager) and PR (Precipitation Radar) over the tropical ocean, and they found that the rainfall peaks around dawn.

The convective index is derived from the infrared (IR) brightness temperature (TBB) because the satellite IR sensor is a measure of the temperature of the cloud top. Short and Wallace (1980) and Murakami (1983) studied the diurnal variation of convection using satellite data, which showed an increase of convective activity in the afternoon over the islands and a maximum convection in the morning over the Pacific Ocean. Hendon and Woodberry's (1993) investigation for the global ocean using IR images showed that the maximum frequency of convection occurred in the early morning. Albright et al. (1985) and Janowiak et al. (1994) compared the diurnal variation of tropical convection determined from the threshold value of IR TBB. These results showed that the moderately cold cloud over the ocean peaked in the afternoon but the deep convection peaked at dawn. Hall and Vonder Haar (1999) analyzed the GMS IR for the West Pacific Ocean during the summer and winter of 1994, and found a diurnal cycle affected by the deep convections in the early morning.

The diurnal variation of convection over the land and coastal regions having an afternoon-early evening maximum is understood as arising from the boundary layer heating in the daytime and the land and sea breeze circulation. As thermal properties of the surface and the effects of boundary heating in the open ocean are not significant, the mechanism responsible for the diurnal cycle of the nocturnal deep convection in the Tropics has yet to be understood (Chen and Houze, 1997).

Previous hypotheses for the diurnal variation over the ocean are in general based on the interactions of static stability, cloud-radiation interaction, and the life cycle of clouds. Kraus (1963) interpreted that during the nighttime, the top of the clouds cool to a larger extent than the cloud base does, and the resulting instability produces vertical overturning. Solar radiation warms and stabilizes the clouds during the daytime. Even though the above explanation is satisfactory for the diurnal cycle of shallow convection, limitations still exist, keeping it from being a proper explanation for the observed large diurnal cycle in the deep convections (Gray and Jacobson, 1977; Tao et al., 1996).

Gray and Jacobson (1977) suggested that the radiational differences between the cloudy and clear regions enhance the deep convective clouds during the nighttime. Sui et al. (1997, 1998) hypothesized that the nocturnal rainfall maximum is associated with a large scale destabilization in the clear regions by the radiative heating-cooling cycle and the resultant change in the available precipitable water.

The cloud-radiation mechanism explaining the diurnal cycle of deep convection assumes a prior condition of the existence of a large cloud system. Simulations of mesoscale convective systems during daytime conditions produce ∼0–7% less surface rainfall than during nighttime conditions. This difference is too small to account for the observed diurnal cycle of precipitation of ∼25%–100% (difference of rainfall amount between 0700 LST and 1900 LST). The amplitude of the diurnal cycle is large for the heavy rainfall period, but on the other hand, the radiative effect on the rainfall is weaker when the large-scale dynamical forcing is strong (Miller and Frank, 1993; Tao et al., 1996; Chen and Houze, 1997).

A hypothesis of the cloud life cycle proposed by Chen and Houze (1997) is based on the result that the larger the cloud size and rainfall, the stronger the magnitude of diurnal variation with a maximum in the early morning (Gray and Jacobson, 1977; Mapes and Houze, 1993). The relationship between tropical rainfall and large-scale motion was shown in Reeves et al. (1979) over the Atlantic Ocean. By analyzing the GATE and Winter Monsoon Experiment (WMONEX) data, Gruber (1976) and Johnson and Priegnitz (1981) examined the diurnal cycle for the disturbed and undisturbed periods defined by the large-scale forcing and found that the amplitude of diurnal variation increased during the disturbed period, and that the phase distribution is nearly the same for both periods. Sui et al. (1997) showed that the deep convection was enhanced at dawn during the disturbed period and shallow convection occurred in the afternoon during the undisturbed period over the Intensive Flux Array (IFA) of Tropical Ocean Global Atmosphere/Coupled Ocean-Atmosphere Response Experiment (TOGA/COARE). Chen and Houze (1997) suggested that a mesoscale convective system tends to form in the afternoon under the warmest ocean surface and atmospheric surface layer, which then evolves into deep convective clouds throughout the night with a life cycle of 18–24 hours.

The characteristics of the diurnal variation of tropical convection seem to be sensitive to the geographical location and large-scale environment causing convection. Thus we analyze the temporal and spatial

variability of the diurnal variation of tropical convection using the surface observation rainfalls and satellite data during the Intensive Observation Period (IOP) of TOGA/COARE. For investigating the large-scale environment in the development of clouds, we compare the kinematic and thermodynamic activities for different time periods.

Section 2 describes the data, and vertical profiles of the kinematic and thermodynamic variables are shown in section 3 to investigate the atmospheric environments for different large-scale regimes. The diurnal variation contained in the time series of the satellite and rainfall observations is shown in section 4, and the conclusion is given in section 5.

2. Data

The data used in this study are based on the TOGA COARE observations for the period November 1992-February 1993. The GMS (Geostationany Meteorological Satellite) IR TBB, rain rates by radar, and rainfall amounts observed by rain gauges on the islands are analyzed to study the diurnal variation of tropical convection. The TOGA COARE objective analysis data are used to analyze the kinematic and thermodynamic variables. A detailed description for each dataset is given in the following.

2.1 *GMS-4 IR TBB and rainfall*

GMS-4 IR TBB has a $0.1^\circ \times 0.1^\circ$ spatial resolution and a 1-hour temporal resolution. The observation domain shown in Fig. 1 covers 15°S–15°N and 130°E–180°.

TBB estimated by the satellite IR sensor has been used as an index for convective activity. Mapes and Houze (1993) suggested that the coverage of cloud colder than 208 K gave an approximate correspondence to the radar echo patterns during the Equatorial Mesoscale Experiment (EMEX), and the area of 208 K cloud top temperature also indicates the rain area derived from SSM/I (Liu et al., 1995). Thus, the 208 K threshold is used for assessing the diurnal variation of convections observed from the satellite during the TOGA COARE IOP.

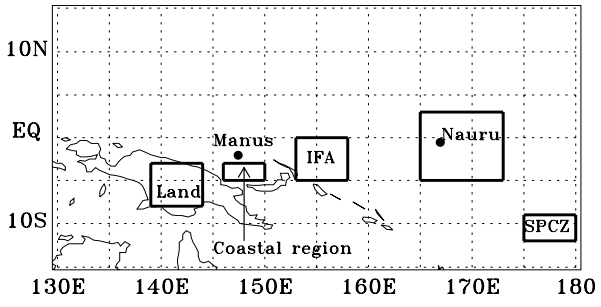

Fig. 1. The entire domain denotes the TOGA COARE GMS data coverage. Black dots represent the rain gauge observation sites on the islands of Manus and Nauru. The thick small rectangles indicate sub-regions for the study of local diurnal variations in the time series of the GMS IR TBB.

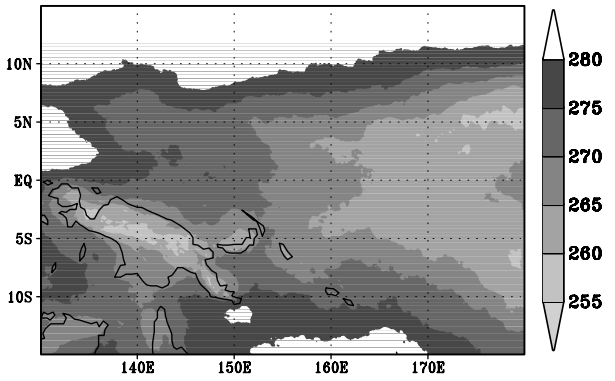

Fig. 2. Time mean values of the GMS IR TBB for the TOGA COARE IOP lasting for four months from November 1992 to February 1993. The shading is in 5°K intervals with the scale shown on the right-hand side of the figure.

The rain rate observed by two radar sets, which were installed on a research vessel in the IFA, is analyzed for the diurnal variation of rainfall. The rain rate used in this study was released from the National Aeronautic and Space Adminstration (NASA) Goddard Space Flight Center by applying the Z-R relations based on the Kapingamarangi Atoll observations (Short et al., 1997). The gridded rain map is within a $5^\circ \times 5^\circ$ latitude-longitude area with a 2-km spatial resolution centered at 2.5°S, 155.5°E.

Rainfall is observed at four islands–Kapingamarangi Atoll, Kavieng, Manus, Nauru–by tipping-bucket rain gauges during the TOGA COARE IOP. Although optical rain gauges were used to observe the rain rate on ships and buoys, they are excluded in this study because of the irregular spatial distribution due to the cruising of ships, in addition to the lack of confidence in the unverified data.

The time mean distribution of GMS IR TBB during the TOGA COARE IOP shows that the convective activity was stronger in the mid-Pacific than in the western Pacific (Fig. 2). Manus Island, which was located in the weak convective region, and Nauru Island, in the active convective region, are chosen to examine the diurnal variability in relation to the degree of convective activity. Manus is a rather large island among the four islands, whereas Nauru is sufficiently small, so that it is possible to investigate the dependence of diurnal variation of rainfall amounts on the size of the

islands for comparison with the results of Gray and Jacobson (1977).

2.2 *Objective analysis for the TOGA COARE IOP*

The TOGA COARE objective analysis data obtained from Colorado State University are analyzed to investigate the kinematic and thermodynamic characteristics of the large-scale environment. The data cover the TOGA COARE Large Scale Array (LSA, 10°S–10°N, 140°E–180°) with a resolution of 1° × 1° and are interpolated vertically from 1000 to 25 hPa with an interval of 25 hPa with rawinsonde data (Lin and Johnson, 1996a).

The data are comprised of wind, temperature, geopotential height and specific humidity. The horizontal convergence, vertical velocity, and heat source / moisture sink are calculated for the kinematic and thermodynamic analysis. The vertical velocity is calculated by the kinematic method, whereas the apparent heat source (Q1) and moisture sink (Q2) are computed using the method of Yanai et al. (1973).

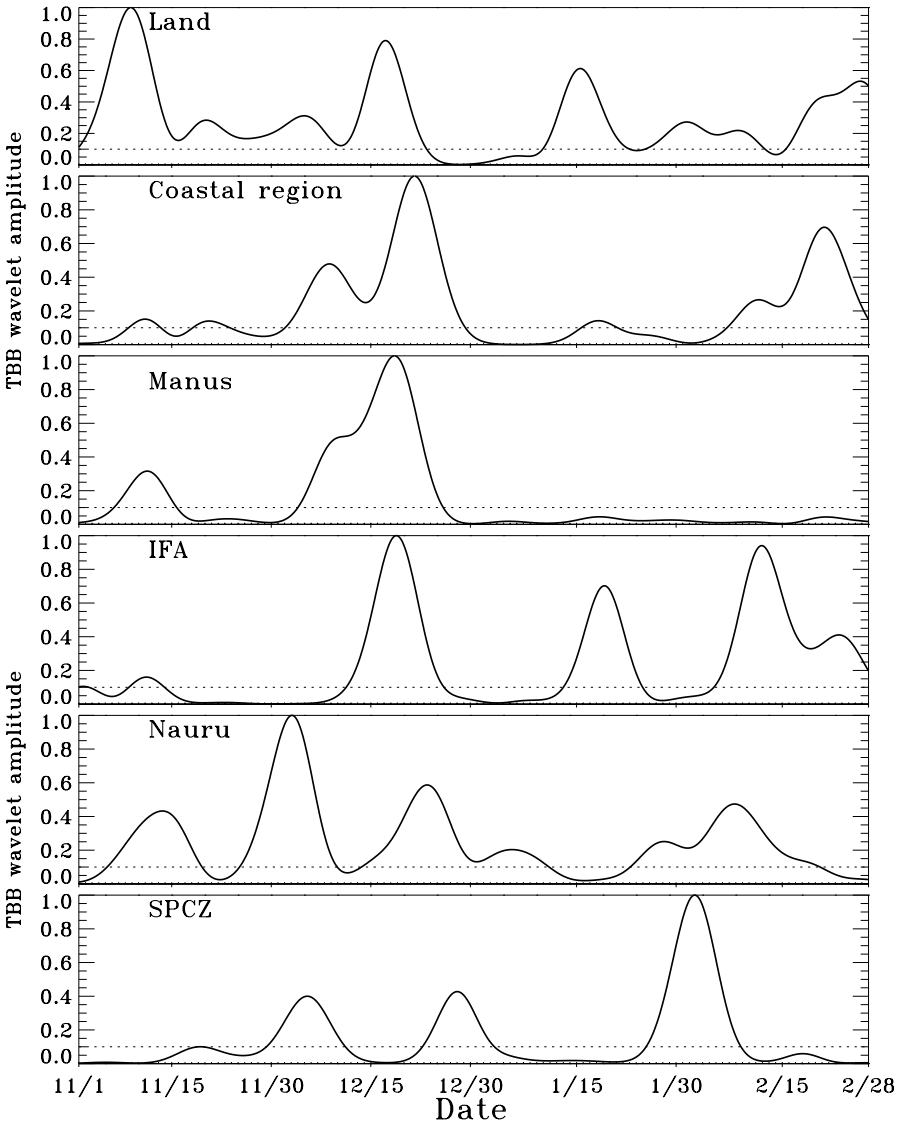

Fig. 3. Normalized wavelet amplitudes with periods of 3–6 days, which are estimated from the time series of PHC_{208}. An active period is defined to have amplitudes larger than or equal to 0.1 in magnitude, denoted by the horizontal dotted lines. The other periods are regarded as inactive periods.

3. Vertical profile of kinematic and thermodynamic variables

Tropical convection appears to be closely related with large-scale motion or circulations such that the MJO modulates a high frequency convection (Reeves et al., 1979; Sui and Lau, 1992; Kiladis et al., 1994). Thus, we analyze the kinematic and thermodynamic variables for different phases of cloud development.

To examine the diurnal variation of the kinematic and thermodynamic fields during the different large-scale regimes, the convective periods are divided into active and inactive periods by applying wavelet analysis to the time series of percent high cloudiness (PHC) with TBB less than 208 K over IFA. The PHC is calculated as the percentage of pixel numbers colder than a threshold temperature at each pixel for a given area. The PHC_{208} was used to denote the fractional coverage of clouds with an IR temperature colder than 208 K (Chen and Houze, 1997). The practical wavelet analysis method used in this study was adopted from Torrence and Compo (1998). Using the above method, we define the active period as having the normalized wavelet power greater than 0.1 for the synoptic disturbances with periods of 3–6 days, which are significant in the Western Pacific (Takayabu and Nitta, 1993), while the remaining periods are classified as inactive periods (Fig. 3).

The vertical profiles of average divergence for the convectively active and inactive periods are shown in Fig. 4a. A significant difference between the convectively active and inactive periods is discernable in the vertical depth of convergence. The convergence extends up to 400 hPa during the convectively active period, but reaches less than about 600 hPa during the inactive period. Vertical velocity during the convectively active period is stronger than that of the inactive period in the mean profile (Fig. 4b). During the convectively active period, the maximum upward vertical motion appears in the upper troposphere (400 hPa). The vertical velocity of strong upward motion in the upper troposphere during the active period and that of shallow upward motion in the inactive period are in agreement with the vertical distribution of convergence.

The profiles of the specific humidity perturbation are shown for both periods, which are clearly contrasted in the middle troposphere. The positive anomaly appears during the active period and shows its maximum between 500 hPa and 700 hPa. The negative anomaly of specific humidity, however, appears in the middle troposphere during the inactive period, and the maximum amplitude of the positive anomaly appears in the lower troposphere around 800 hPa (Fig. 4c). The largest difference in specific humidity appears in the middle troposphere in periods with convectively active cloud clusters and in fair weather in the analysis of Lucas and Zipser (2000).

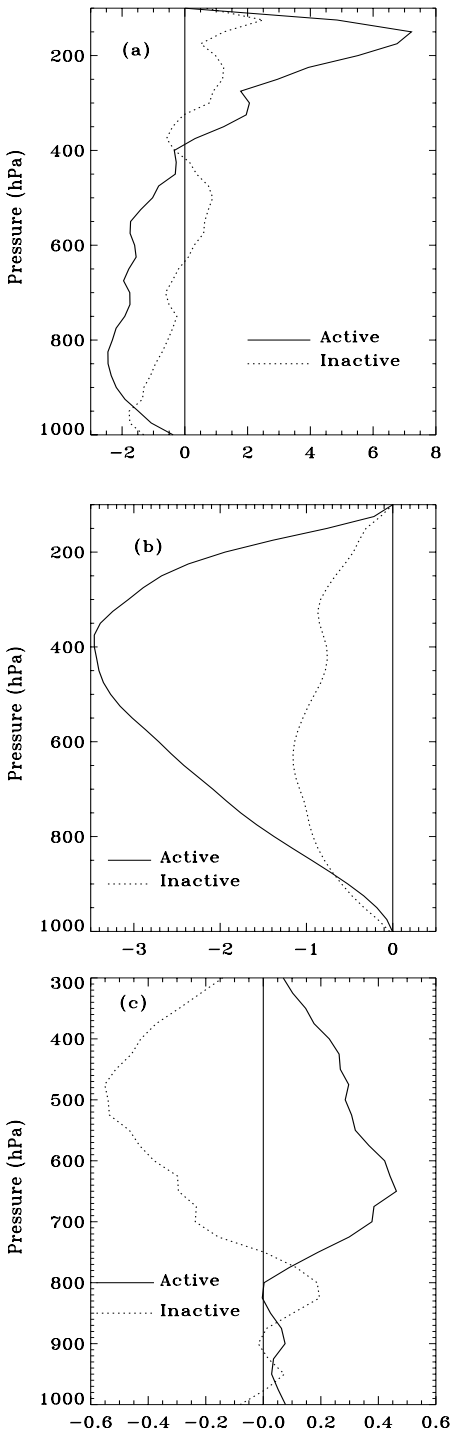

Fig. 4. Vertical profile of (a) divergence (10^{-6} s^{-1}), (b) vertical velocity (hPa h^{-1}), and (c) specific humidity perturbation (g kg^{-1}) over the IFA during the convectively active and inactive periods.

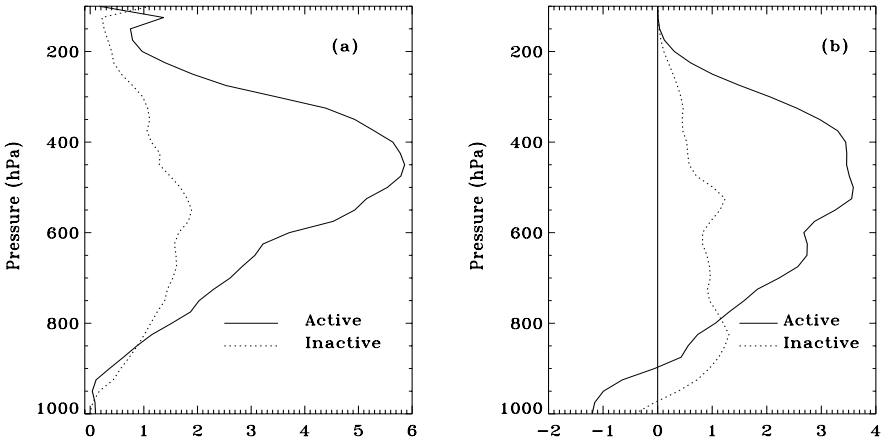

Fig. 5. As in Fig. 4, but (a) is for the heat source (K d^{-1}) and (b) is for the moisture sink (K d^{-1}).

The difference of the cloud height between the convectively active and inactive periods appears in the distribution of the heat source (Fig. 5a). The heat source exhibits its maximum near 450 hPa during the active period, compared to around 650 hPa during the inactive period. The moisture sink peaks between 400 hPa and 500 hPa, where the associated condensation is maximized during the active period. The heights of the maxima of the moisture sink during the inactive period appear around 500 hPa and 850 hPa (Fig. 5b).

Heating and moisture sink profiles over the western Pacific Ocean have been investigated by many authors (Yanai et al., 1973; Lin and Johnson, 1996b; Yang and Smith, 1999; Yang and Smith, 2000). Our maximum heating rate between 400 hPa and 450 hPa during the convectively active period is consistent with the mean heating rate profile of IOP over the IFA from Lin and Johnson (1996b). By the way, the moisture sink curve over the IFA from Lin and Johnson (1996b) has a different feature in contrast with Yanai et al. (1973) that indicates two peaks at 700 hPa and 500 hPa. The double peak structure in the inactive period of Fig. 5b is consistent with Yanai et al. (1973). Johnson (1984) proposed that the double peak structure is a combined consequence of two different drying phenomena. He suggested that the lower peak is a result of cumulus updrafts in the convective region, while the upper one comes from the mesoscale updraft within the anvil clouds. Although there exist differences in the magnitudes of the moisture sink, the distribution in the convectively active period is similar to the IOP mean profile by Lin and Johnson (1996b), which indicates the moistening below 900 hPa. This moistening is due to strong evaporation and upward transport of moisture by shallow cumuli (Lin and Johnson, 1996b).

Yang and Smith (1999, 2000) studied a heat source and moisture sink for convective and stratiform cases. For the convective systems, the heat source and moisture sink are positive throughout the troposphere. In the stratiform systems, the profile of the heat source indicates a cooling process below 650 hPa and a heating process up to 250 hPa with a maximum value around 400 hPa. The profile of the moisture sink suggests moistening below 700 hPa and drying above that level with a maximum near 450 hPa (Yang and Smith, 1999; Yang and Smith, 2000). Compared to Yang and Smith (1999, 2000), the peak of the heat source at 400 hPa during the convectively active period may result from mesoscale updrafts within anvil clouds and the weakening of the heating during the inactive period comes from the updraft by cumulus, while the cooling below 650 hPa shown in Yang and Smith (1999, 2000) is not observed in our analysis. Although the altitude of moistening is low during the convectively active period, the maximum drying at 400–500 hPa is similar to the stratiform systems in Yang and Smith (1999, 2000). The difference in features of heat source and moisture sink profiles with Yang and Smith (1999, 2000) may result from using the classification method of PHC_{208}. Now PHC_{208} is not for classification of cloud type, but for cloud development. Due to the intrinsic problem of classifying the convective period with PHC_{208}, cases of the convectively active period including anvil cloud and small cumulus are abundant in the inactive period.

Sensitivity tests on the criterion of wavelet power magnitude have been conducted to examine its effects on profiles by classification of the convectively active and inactive periods (not shown). As the threshold value increases, the change in the vertical distribution is significant for the convectively inactive period rather than for the active period. For the former, the conver-

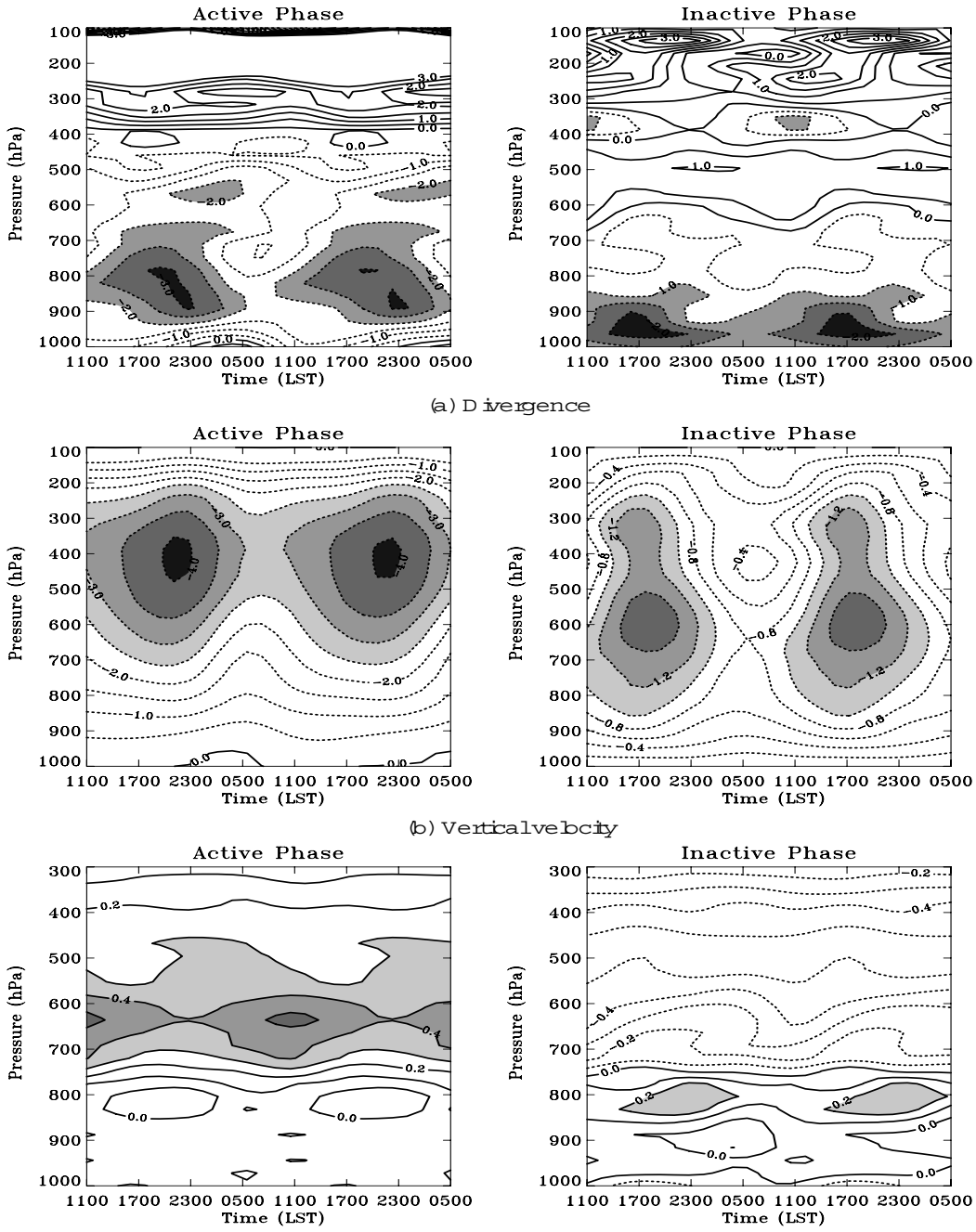

Fig. 6. Diurnal variation of (a) divergence with contours with 0.5×10^{-6} s^{-1} intervals, (b) vertical velocity with contours with 0.5 hPa h^{-1} intervals for the active period and 0.2 hPa h^{-1} intervals for the inactive period, and (c) specific humidity perturbation with contours with 0.1 g kg^{-1} intervals over the IFA during the convectively active and inactive periods.

gence layer and height of maximum upward motion increase as the threshold value is raised. Higher threshold values cause a decrease of negative perturbation in the specific humidity and an increase of maximum height in the profile of the heat source. The double peak structure of the moisture sink profile with a drying maximum around 800 hPa and 500 hPa is a similar feature in the 0.1 threshold.

The diurnal variation of divergence shows the maximum convergence near 850 hPa at 2300 LST during

the convectively active period. In contrast, there is a convergence peak around 950 hPa at 1700 LST during the inactive period, and the convergence decreases in the evening. The level of maximum convergence is lower during the inactive period than in the active period (Fig. 6a).

The maximum of vertical motion at 2300 LST during the convectively active period may be associated with the middle troposphere convergence feature (Fig. 6b). During the inactive period, a peak is shown at 1700 LST, around 600 hPa. The convectively active period is dominated by deep convective effects with a strong convergence up to 400 hPa around midnight and a strong upward motion in the upper troposphere. On the other hand, the convergence maximum is placed in the lower troposphere in the afternoon with a weak upward motion during the inactive period.

As in the divergence and vertical velocity, a distinct diurnal oscillation of specific humidity appears with a morning maximum (1100 LST) during the convectively active period. The specific humidity is considerably weaker during the inactive period than the active period in the middle troposphere, and has a maximum at 850 hPa in the afternoon and evening (1700–2300 LST) (Fig. 6c).

The diurnal cycle of the heat source is similar to the specific humidity such that the largest value of the heat source is found near 0500–1100 LST during the convectively active period and near 1100–1700 LST during the inactive period (Fig. 7a). A maximum moisture sink appears at midnight and dawn (2300–0500 LST) due to the condensation of water vapor during the convectively active period, while it occurs between 1700 LST and 0500 LST in the low troposphere during the inactive period (Fig. 7b).

4. Diurnal variation of tropical convection

4.1 *Diurnal variation in satellite observations*

Figure 8 shows the IOP mean cloud coverage deriv-

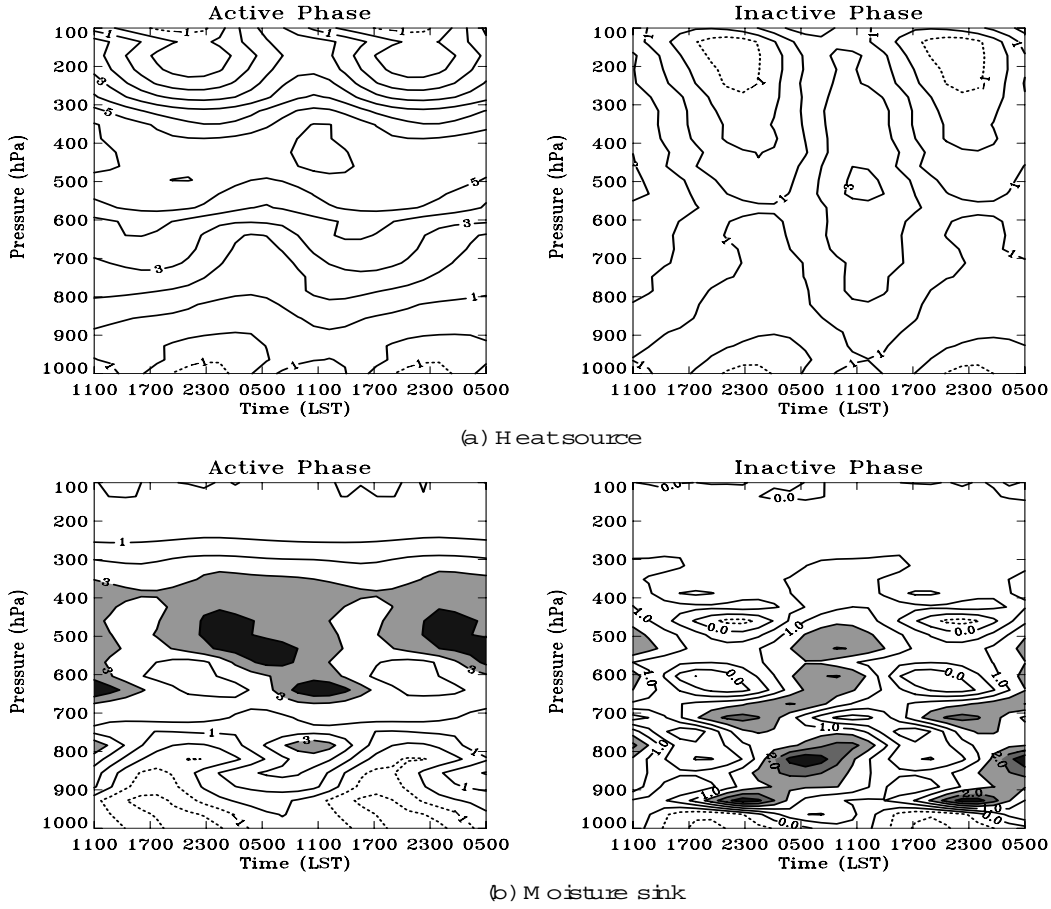

Fig. 7. As in Fig. 6, but (a) is for the heat source with contours with 1 K d^{-1} intervals and (b) is for the moisture sink with contours with 1 K d^{-1} intervals for the active period and 0.5 K d^{-1} intervals for the inactive period. Negative values are dashed.

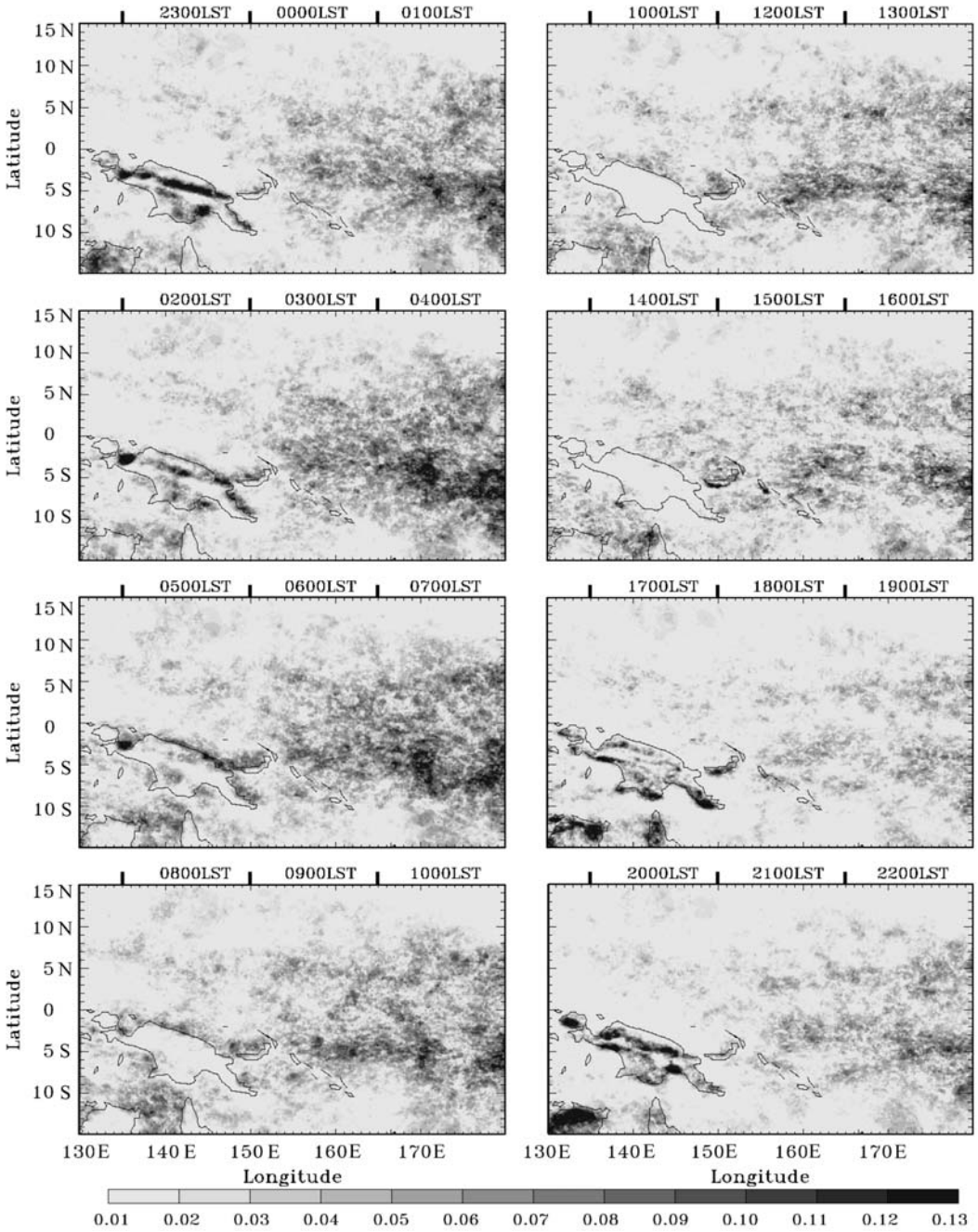

Fig. 8. Diurnal variation in the ratio of cloud coverage estimated from GMS IR TBB lower than 208 K for the TOGA COARE IOP lasting for four months from November 1992 to February 1993.

ed from IR TBB colder than the 208 K threshold (PHC_{208}). A significant phase difference is observed between the diurnal variation over land and that over the ocean. Over land, a convection is found with a maximum around midnight (2300 LST) and a minimum at 0800–1400 LST, while the strongest convective activity occurs at 0100–0700 LST and the weakest at 1800–2100 LST over the mid-Pacific Ocean (15°S–10°N, 160°E–180°).

To identify and describe a periodic variability of fractional coverage on a regional basis, a spectral analysis is performed for the PHC_{208} time series of Papua New Guinea, the costal region of Papua New Guinea, Manus, IFA, Nauru and the SPCZ. During the TOGA COARE IOP, the mean TBB is colder over the mid-Pacific region than in the western Pacific as shown in Fig. 2. This may be due to the location of the ITCZ.

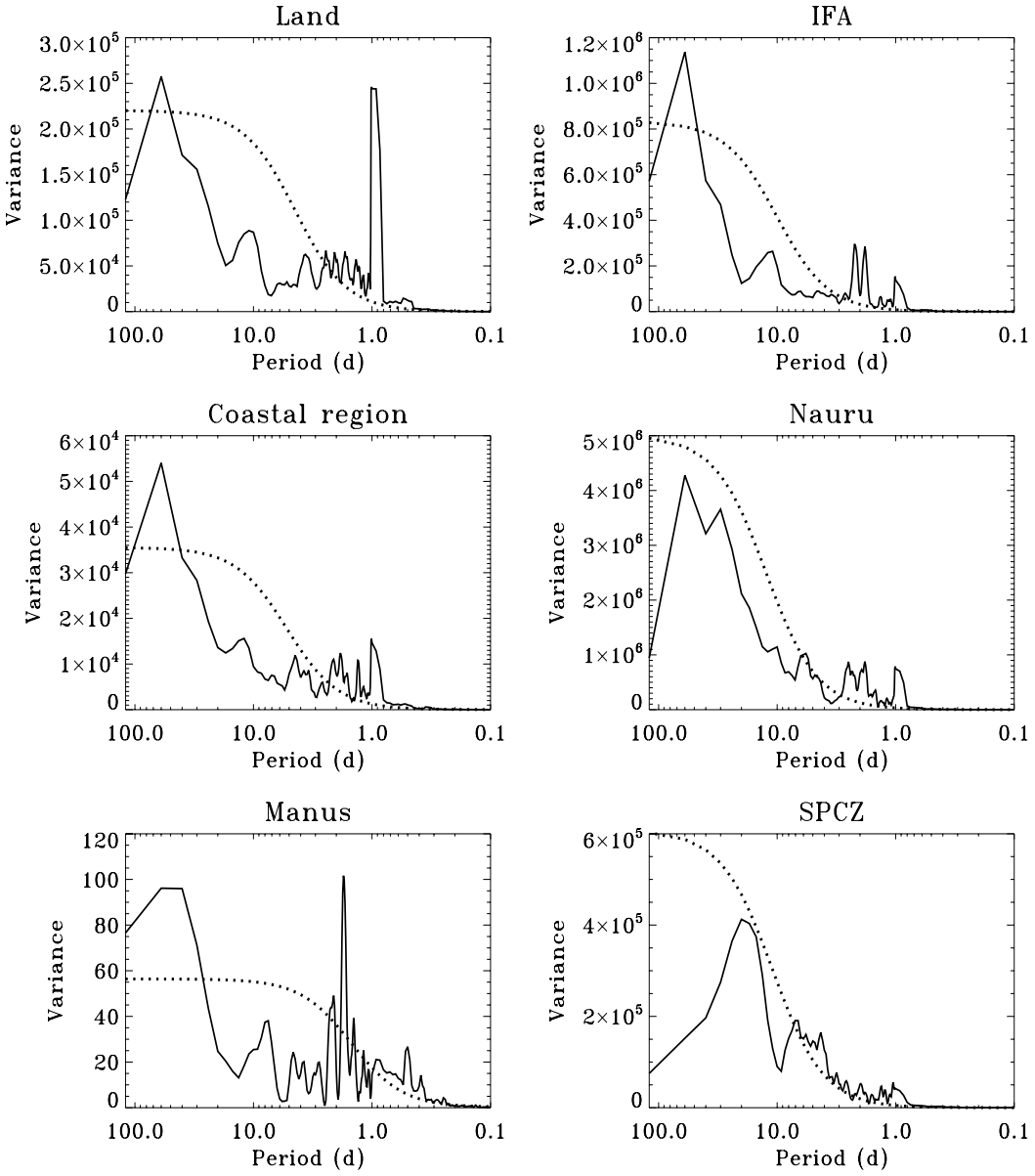

Fig. 9. Power spectra of the time series of the fractional coverage of clouds defined with their top temperature colder than 208 K. Dotted curves indicate the spectra of the corresponding red noise functions.

The diurnal variation of the convection around Nauru, which is located in the strong convective region, may stand for the diurnal variation in the ITCZ. The diurnal variation of Manus Island may represent that of the weak convective region.

The results of the spectral analysis show the multiscale variations over the TOGA COARE domain (Fig. 9). This result is consistent with the previous studies by Weng and Lau (1994) and Chen et al. (1996). They said that the convective activity over the western tropical Pacific Ocean included the short-period oscillations embedded in the intraseasonal oscillation.

It is observed that there are diurnal variations in the activity of deep convection around Papua New Guinea and its coastal region. Semidiurnal and 2-day oscillations are apparent at Manus Island (Fig. 9). The 2-day period component is reduced and the 1-day period is distinctive in the analysis of the cloud coverage between 273 K and 288 K (warm clouds) of Manus Island as shown in Fig. 10.

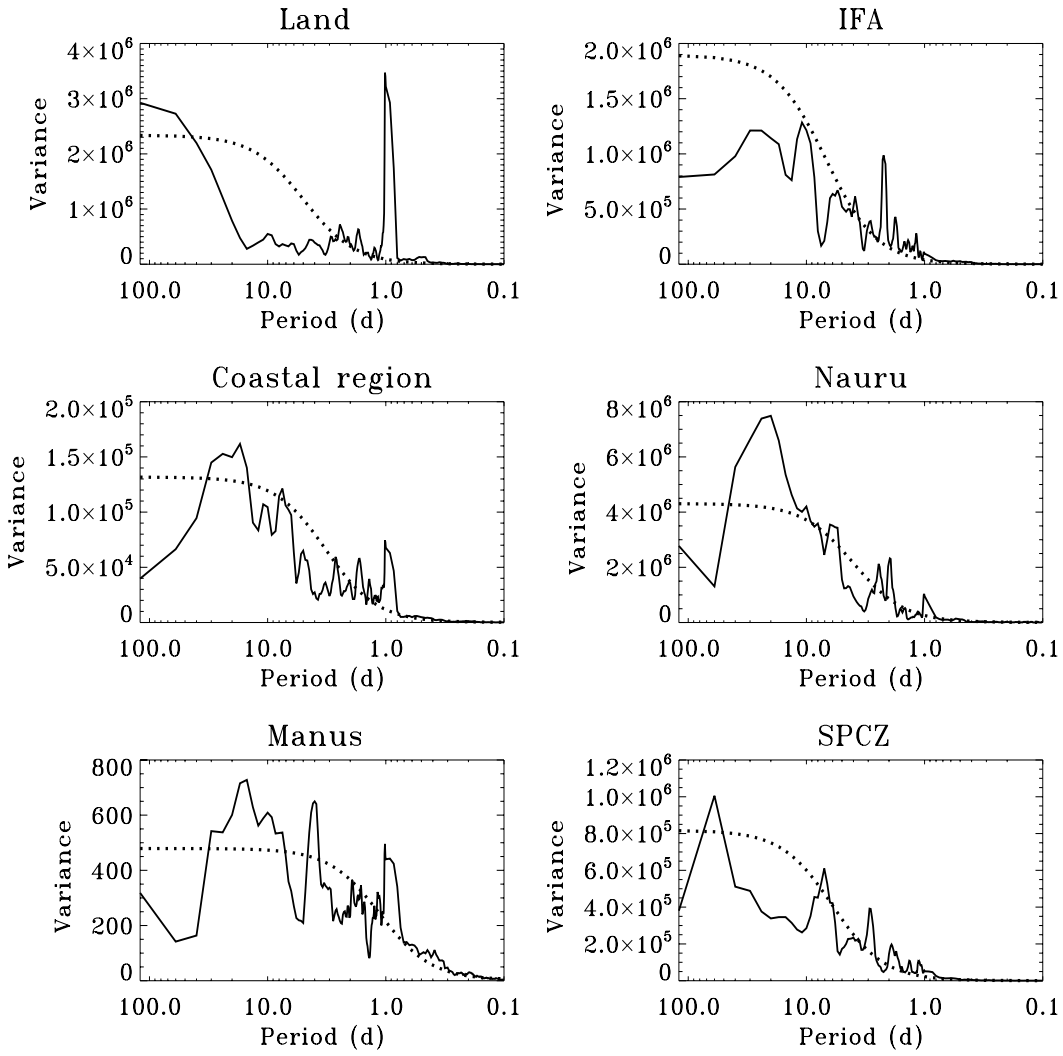

Fig. 10. As in Fig. 9, but for the warm clouds, for which the TBB is between 273 K and 288 K.

Spectral analysis of the fractional coverage of deep convection over Nauru and the IFA shows the diurnal and 2-day period spectral peaks. The 2-day period peak is stronger than the diurnal peak for the fractional coverage of warm clouds. This feature is also observed over the SPCZ, in which the 2-3-day period peak is stronger than the 1-day peak for the warm clouds (Fig. 10). It seems that these facts are related with the life cycle of the convective clouds over the tropical ocean. It can be inferred that the cloud life cycle of Nauru and the SPCZ is longer than those of the land where clouds develop and decay with a one-day cycle.

To examine the effects of the degree of convective activity on the diurnal variation of convection, the temporal variation is classified as in Fig. 3. The distribution of TBB histogram anomalies during the active period shows that the land and the coast display opposite features. The high clouds (TBB <233 K) over the land are extended at midnight (2200 LST) and decay during the dawn and afternoon. The midlevel (233 K<TBB<273 K) and warm clouds (273 K<TBB) are maximized in the morning and at noon. On the other hand, the maximum presence of high clouds over the coastal region develops at dawn (0600 LST), while the midlevel clouds may be observed in the afternoon and early evening. The warm clouds appear in the morning over the coastal region. At Manus Island, the high clouds show a semidiurnal variation with afternoon and dawn peaks. Spectral analysis reveals a semi-

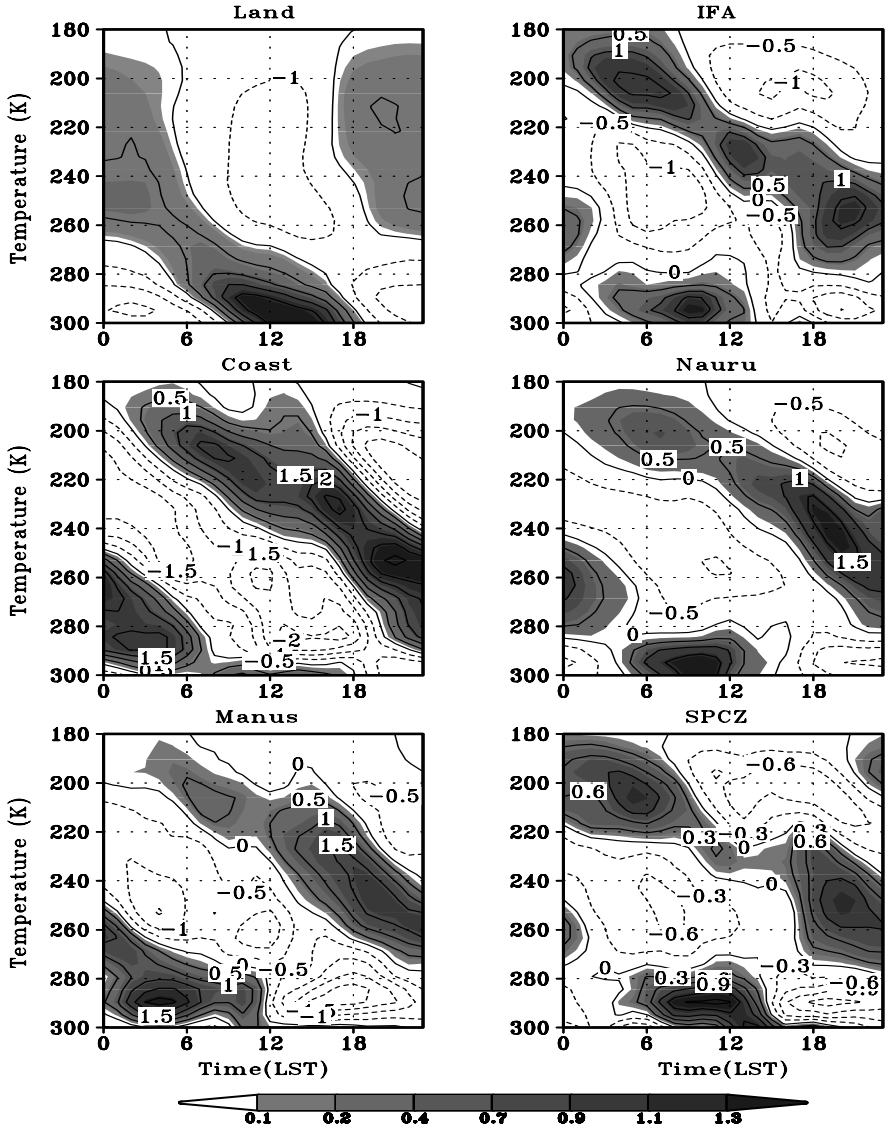

Fig. 11. Diurnal variation of the histogram of TBB anomaly for the convectively active period of the TOGA COARE. Positive-value areas are shaded to denote the development of cloud.

diurnal peak that is stronger than the diurnal peak at Manus Island. The warm clouds appear most frequently in the early morning at Manus (Fig. 11).

In Fig. 11, the diurnal variation of high clouds for the oceanic region such as the IFA, Nauru, and the SPCZ shows that the high clouds develop in the early morning at 0400–0800 LST and gradually decrease in the afternoon. The midlevel clouds are observed in the afternoon and at midnight.

The diurnal variation of convection during the convectively inactive period over land and coastal regions is similar to the active period, but the convective intensity is weaker than in the active period. Convection develops in the afternoon, and nocturnal convection does not appear on Manus Island. The TBB histogram anomalies during the inactive period over the oceanic regions such as the IFA, Nauru, and the SPCZ shows that the high clouds develop in the afternoon, with the midlevel and warm clouds at dawn (Fig. 12).

The observed diurnal variation of tropical convection during TOGA COARE is contrasted between the land and ocean. The diurnal variation in the active period is almost similar to that in the inactive period over the land region, while the open ocean shows that the deep convection increases at dawn during the active period and in the afternoon during the inactive

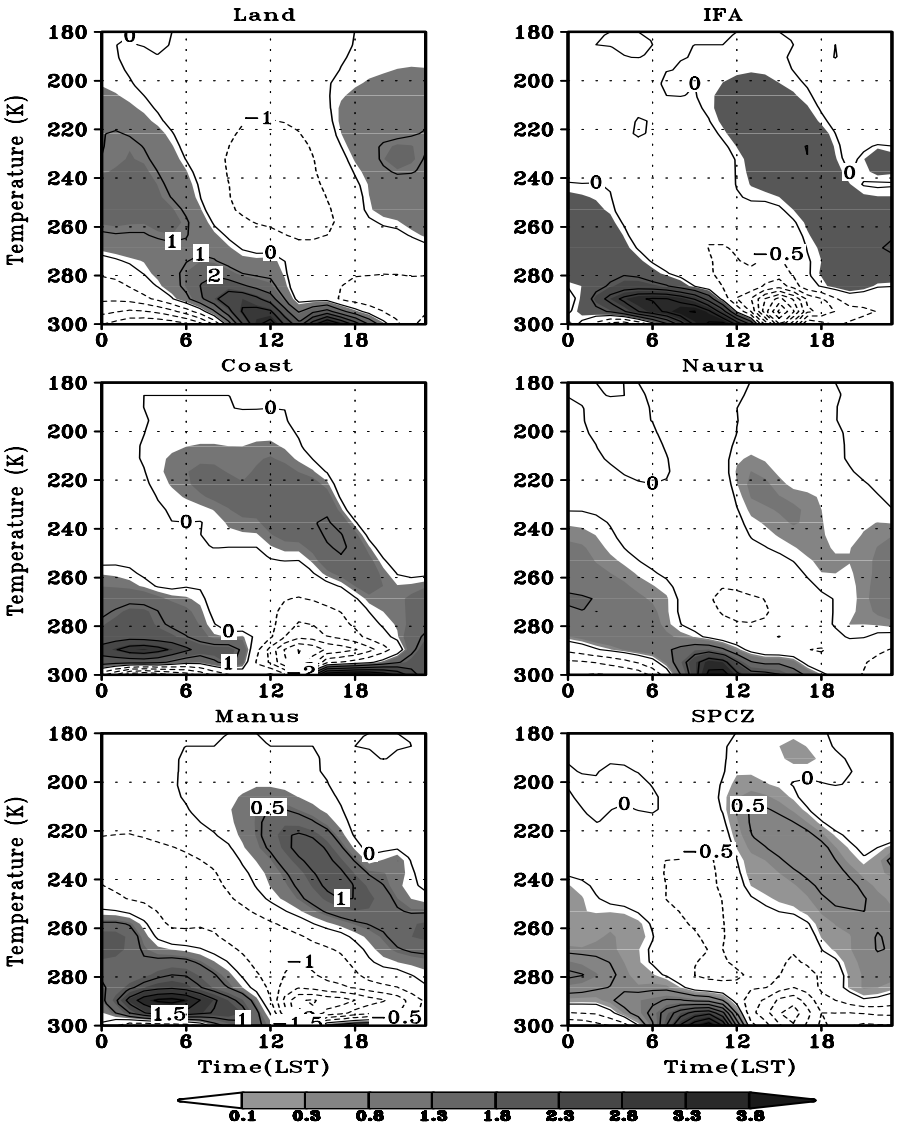

Fig. 12. As in Fig. 11., but for the inactive period of convection.

period. The diurnal variation in the western Pacific Ocean is different from that of Africa and South America which is characterized by afternoon maximum convection (McGarry and Reed, 1978; Mapes et al., 2003). The maximum time of convection over the land and coastal regions is influenced by the sea-land contrast and topography, but the different features of diurnal variation over the open ocean according to the convective period may be caused from the large-scale environment.

4.2 *Diurnal variation in the rainfall amounts*

Multiscale variabilities are discernable in the spectral analysis of surface observations of rainfall amounts (Fig. 13). The 1-day period is the most pronounced in the rainfall of Manus and Nauru. Peaks with periods of 2–3-, 6-, 30- and 40-days are shown. The radar rain rate observed for the IFA also shows significant spectral peaks in the high frequency range of 1 and 2–4 days, besides the low frequency components.

In Fig. 14, the diurnal variations of rainfall amounts during the TOGA COARE IOP may be distinguished in that an afternoon peak of diurnal variation occurs at Manus. In contrast, an early morning peak from midnight to 0800 LST is dominant at Nauru and in the IFA. The diurnal variation of rainfall amount is consistent with the diurnal variation of GMS IR TBB in that a convection is developed in the afternoon over Manus and at dawn over Nauru and the IFA. A weak rainfall peaks at dawn and during the af-

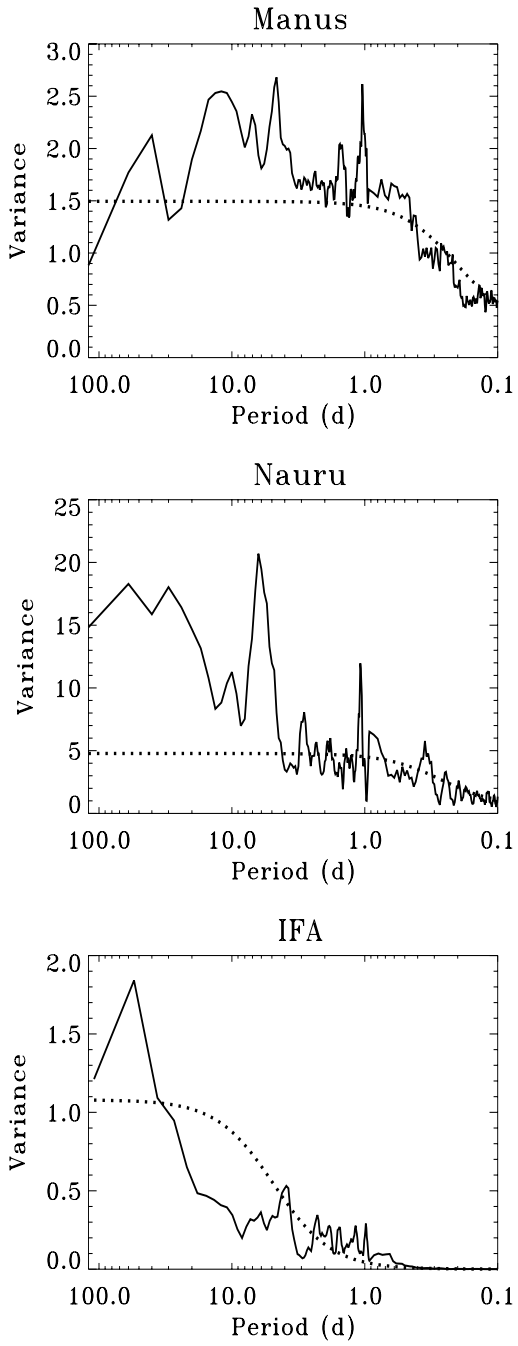

Fig. 13. Power spectra of the observed rainfall amounts at Manus, Nauru, and IFA for the TOGA COARE IOP. Dotted curves denote the spectra of the respective red noise functions.

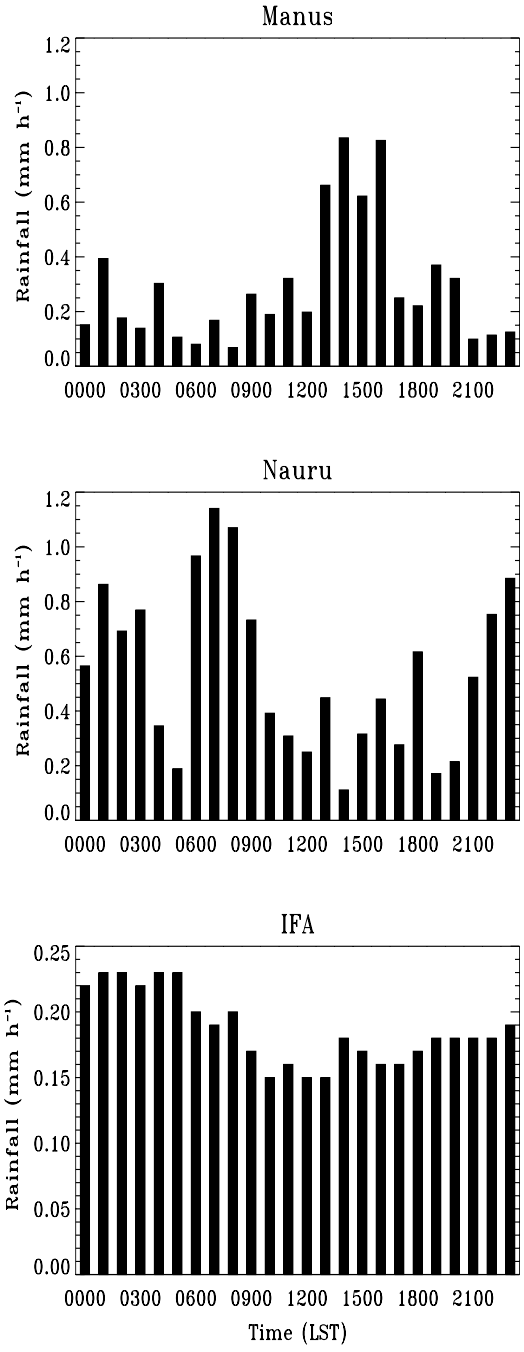

Fig. 14. Diurnal variation of four-month averages of rainfall, which were observed at Manus, Nauru, and over the IFA for the TOGA COARE IOP.

ternoon on Manus, which is consistent with Gray and Jacobson's (1977) finding of a semidiurnal oscillation and a stronger afternoon peak over a larger island.

From the difference of the maximum rainfall time over Manus and Nauru, we can infer that the diurnal variation of rainfall is influenced by the temporal and regional variation of cloud development. Thus, in order to examine the diurnal variation of the rainfall amount in a different large-scale environment, the convectively active and inactive periods are divided by using the wavelet analysis of PHC_{208}.

The amount of rainfall at Manus peaks at 1300–1600 LST during the convectively active and inactive

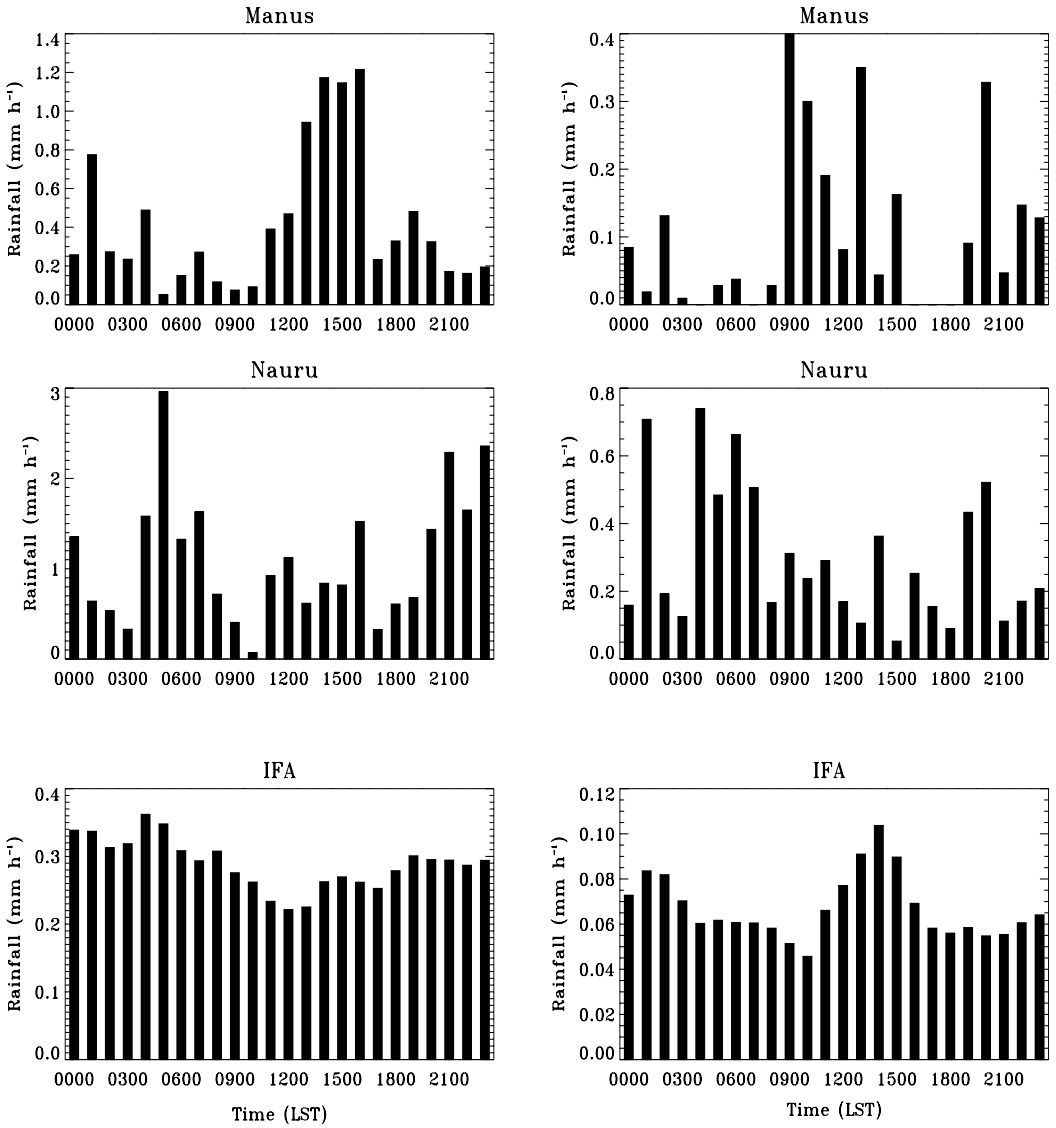

Fig. 15. Diurnal variation in the time series of the hourly amounts of rainfall for the convectively active period in the left-hand side column panels and for the inactive period in the right-hand panels.

periods, but the rainfall at Nauru shows a maximum at dawn in both periods. The diurnal variation of rainfall amount under a different large-scale regime over the IFA is clearly different. The rain rate has a peak at dawn during the convectively active period, and maximum rainfall appears in the afternoon during the inactive period (Fig. 15). The reason for this difference is due to the cloud cluster and the precipitation mechanism. The weekly mean TBB distribution shows that large convective clouds are seldom observed at Manus during the TOGA COARE IOP, and that large cloud clusters associated with the ITCZ are almost static at Nauru. Over the IFA region, a large cloud cluster forms in the active period, while small clouds are found frequently during the inactive period (not shown). Therefore, the precipitation is caused from the small scale and short time period of cloud at Manus, from a large cloud cluster at Nauru, and from the small-scale cloud to the large-scale cloud cluster over the IFA.

5. Conclusions

The diurnal variation of tropical convection in the different large scale environments during the TOGA COARE IOP has been investigated by using the sur-

face observations of rainfall amounts, radar rain rates, and the GMS-4 IR TBB. Large-scale environments are classified into convectively active and inactive periods by using the results from a wavelet analysis of the time series of TBB colder than 208 K. To examine the kinematic and thermodynamic characteristics of the classified large-scale environments, we used the vertical profiles of variables derived from the TOGA COARE objective analysis data.

Over the IFA, the vertical profiles are different in the shape of the kinematic and thermodynamic variables between the convectively active and inactive periods. For the convectively active period, the convergence increases up to the 400-hPa level, with a maximum near 850 hPa at 2300 LST. The upward vertical motion is the strongest in the upper troposphere (400 hPa) at midnight (2300 LST), and the specific humidity perturbation shows a maximum at 600–700 hPa. The vertical profiles of the heat source and moisture sink indicate that the clouds develop in the upper troposphere (450 hPa) with a midnight peak. On the other hand, for the inactive period, the height of the convergence layer is displaced downward with its maximum in the lower troposphere (950 hPa), and the maximum of convergence is found in the afternoon (1700 LST). The upward motion that appears in the afternoon is maximized in the middle troposphere (600 hPa). The specific humidity perturbation shows a peak in the daytime in the lower troposphere and a negative one in the middle troposphere. The altitudes of the maximum values of heat source and moisture sink are lower when compared with those of the convectively active period.

The spectral analyses of the times series of PHC_{208} and rainfall amounts indicate that the high-frequency components of variations with a prominent diurnal cycle coexist with the low frequency components which represent the slowly varying convective activity associated with the large-scale weather conditions. Over land, the diurnal variation of tropical convections is found to have a midnight maximum of amplitude, which is common to the convectively active and inactive periods. Over the ocean, such as in the IFA, ITCZ, and SPCZ regions, the convection reaches a maximum activity level at dawn during the convectively active period, while in the afternoon during the inactive period.

The surface observations of rainfall amounts also show a diurnal variation. Manus Island shows an afternoon maximum of rainfall, but an early morning peak appears in Nauru with a large amount of rainfall. The diurnal variation of rainfall amount based on radar observation over the IFA shows a maximum at dawn during the convectively active period and in the afternoon during the inactive period. Oceanic convections show their peaks at different times of day according to the strength of convective activity. The deep convection in the morning and a shallow one in the afternoon over the ocean are consistent with the results in which the heavier and larger clouds appear at dawn, while light rain and small clouds occur in the afternoon (Gray and Jacobson, 1977; Chen and Houze, 1997).

Comparing the vertical profile of kinematic and thermodynamic fields with the diurnal variation of convection over the ocean, the large-scale variables reflect the diurnal variation of the deep convection at night and the shallow convection in the afternoon. The diurnal variations of the large-scale variables and convection in different periods are evidence for the convective life cycle proposed by Chen and Houze (1997). The deep convective cloud during the convectively active period evolves throughout the nighttime after its initiation in the afternoon.

The role of large scale variables in the development of deep convection may be recognized in Fig. 4, which shows the vertical profile of the specific humidity perturbation. The difference of specific humidity perturbation between the convectively active and inactive periods is significant in the middle troposphere. During the convectively active period, the specific humidity perturbation shows a positive value throughout the entire troposphere with its maximum occurring around 650 hPa, while the positive value is found in the lower troposphere with a maximum at 800 hPa during the inactive period. Brown and Zhang (1997) showed a good correlation between rainfall and relative humidity in the mid to upper troposphere. By a numerical experiment, Ridout (2002) suggested that rainfall was most sensitive to moisture in the mid- to upper-level troposphere. Nocturnal rainfall during the convectively active period results mostly from the cloud system which reaches its maximum in the nighttime after initiation in the afternoon, when sufficient moisture exists in the middle troposphere.

Acknowledgments. The authors would like to acknowledge Dr. Paul E. Ciesielski at Colorado State University for providing the TOGA COARE objective analysis data. Valuable comments from two anonymous reviewers greatly improved the original manuscript. This work was supported by the Korean Government's BK21 and NRL Projects.

REFERENCES

Albright, M. D., E. E. Recker, R. J. Reed, and R. Dang, 1985: The diurnal variation of deep convection and

inferred precipitation in the central tropical Pacific during January-February 1979. *Mon. Wea. Rev.*, **113**, 1663–1680.

Augustine, J. A., 1984: The diurnal variation of large-scale inferred rainfall over the tropical Pacific Ocean during August 1979. *Mon. Wea. Rev.*, **112**, 1745–1751.

Brown, R. G., and C. Zhang, 1997: Variability of midtropospheric moisture and its effect on cloud-top height distribution during TOGA COARE. *J. Atmos. Sci.*, **54**, 2760–2774.

Chang, A. T. C., L. S. Chiu, and G. Yang, 1995: Diurnal cycle of oceanic precipitation from SSM/I data. *Mon. Wea. Rev.*, **123**, 3371–3380.

Chen, S. S., and R. A. Houze Jr., 1997: Diurnal variation and life-cycle of deep convective systems over the tropical Pacific warm pool. *Quart. J. Roy. Meteor. Soc.*, **123**, 357–388.

Chen, S. S., R. A. Houze Jr., and B. E. Mapes, 1996: Multiscale variability of deep convection in relation to large-scale circulation in TOGA COARE. *J. Atmos. Sci.*, **53**, 1380–1409.

Gray, W. M., and R. W. Jacobson, 1977: Diurnal variation of deep cumulus convection. *Mon. Wea. Rev.*, **105**, 1171–1188.

Gruber, A., 1976: An estimate of the daily variation of cloudiness over the GATE A/B area. *Mon. Wea. Rev.*, **104**, 1036–1039.

Hall, T. J., and T. H. Vonder Haar, 1999: The diurnal cycle of West Pacific deep convection and its relation to the spatial and temporal variation of tropical MCSs. *J. Atmos. Sci.*, **56**, 3401–3415.

Hendon, H. H., and K. Woodberry, 1993: The diurnal cycle of tropical convection. *J. Geophys. Res.*, **98**, 16 623–16 637.

Imaoka, K., and R. W. Spencer, 2000: Diurnal variation of precipitation over the tropical oceans observed by TRMM/TMI combined with SSM/I. *J. Climate*, **13**, 4149–4158.

Janowiak, J. E., P. A. Arkin, and M. Morrissey, 1994: An examination of the diurnal cycle in oceanic tropical rainfall using satellite and in situ data. *Mon. Wea. Rev.*, **122**, 2296–2311.

Johnson, R. H., 1984: Partitioning tropical heat and moisture budgets into cumulus and mesoscale components: Implications for cumulus parameterization. *Mon. Wea. Rev.*, **112**, 1590–1601.

Johnson, R. H., and D. L. Priegnitz, 1981: Winter monsoon convection in the vicinity of North Borneo. Part II: Effects on large-scale fields. *Mon. Wea. Rev.*, **109**, 1619-1632.

Kiladis, G. N., G. A. Meehl, and K. M. Weickmann, 1994: Large-scale circulation associated with westerly wind bursts and deep convection over the western equatorial Pacific. *J. Geophys. Res.*, **99**, 18 527–18 544.

Lin, X., and R. H. Johnson, 1996a: Kinematic and thermodynamic characteristics of the flow over the western Pacific warm pool during TOGA COARE. *J. Atmos. Sci.*, **53**, 695–715.

Lin, X., and R. H. Johnson, 1996b: Heating, moistening, and rainfall over the western Pacific warm pool during TOGA COARE. *J. Atmos. Sci.*, **53**, 3367–3383.

Liu, G. S., J. A. Curry, and R. S. Sheu, 1995: Classification of clouds over the western equatorial Pacific Ocean using combined infrared and microwave satellite data. *J. Geophys. Res.*, **100**, 13 811–13 826.

Lucas, C. E., and E. J. Zipser, 2000: Environmental variability during TOGA COARE . *J. Atmos. Sci.*, **57**, 2333–2350.

Mapes, B. E., and R. A. Houze Jr., 1993: Cloud clusters and superclusters over the oceanic warm pool. *Mon. Wea. Rev.*, **121**, 1398–1415.

Mapes, B. E., T. T. Waner, M. Xu, and A. J. Negri, 2003: Diurnal patterns of rainfall in northwestern South America. Part I : Observations and context. *Mon. Wea. Rev.*, **131**, 799–812.

McGarry, M. M., and R. J. Reed, 1978: Diurnal variations in convective activity and precipitation during phases III and II of GATE. *Mon. Wea. Rev.*, **106**, 101–112.

Miller, R. A., and W. M. Frank, 1993: Radiative forcing of simulated tropical cloud clusters. *Mon. Wea. Rev.*, **121**, 482–498.

Murakami, M., 1983: Analysis of the deep convective activity over the western Pacific and Southeast Asia. Part I: Diurnal variation. *J. Meteor. Soc. Japan*, **61**, 60–76.

Nakazawa, T., 1988: Tropical super clusters within intraseasonal variations over the western Pacific. *J. Meteor. Soc. Japan*, **66**, 823–839.

Nesbitt, S. W., and E. J. Zipser, 2003: The diurnal cycle of rainfall and convective intensity according to three years of TRMM measurements. *J. Climate*, **16**, 1456–1475.

Reeves, R. W., C. F. Ropelewski, and M. D. Hudlow, 1979: Relationship between large-scale motion and convective precipitation during GATE. *Mon. Wea. Rev.*, **107**, 1154–1168.

Ridout, J. A., 2002: Sensitivity of tropical Pacific convection to dry layers at mid- to upper levels: Simulation and parameterization tests. *J. Atmos. Sci.*, **59**, 3362–3381.

Short, D. A., and J. M. Wallace, 1980: Satellite inferred morning to evening cloudiness changes. *Mon. Wea. Rev.*, **108**, 1160–1169.

Short, D. A., P. A. Kucera, B. S. Ferrier, J. C. Gerlach, S. A. Rutledge, and O. W. Thiele, 1997: Shipboard radar rainfall patterns within the TOGA COARE IFA. *Bull. Amer. Meteor. Soc.*, **78**, 2817–2836.

Sui, C. -H., and K. -M. Lau, 1992: Multiscale phenomena in the tropical atmosphere over the western Pacific. *Mon. Wea. Rev.*, **120**, 407–430.

Sui, C. -H., K. -M. Lau, Y. Takayabu, and D. Short, 1997: Diurnal variations in tropical oceanic cumulus convection during TOGA COARE. *J. Atmos. Sci.*, **54**, 639–655.

Sui, C. -H., X. Li, and K.-M. Lau, 1998: Radiative-convective processes in simulated diurnal variations of tropical oceanic convection. *J. Atmos. Sci.*, **55**, 2345–2357.

Takayabu, Y. N., and T. Nitta, 1993: 3–5 day-period disturbances coupled with convection over the tropical Pacific Ocean. *J. Meteor. Soc. Japan*, **71**, 221–246.

Tao, W. -K., S. Lang, J. Simpson, C. -H. Sui, B. Ferrier, and M.-D. Chou, 1996: Mechanisms of cloud-radiation interaction in the Tropics and mid-latitudes. *J. Atmos. Sci.*, **53**, 2624–2651.

Torrence, C., and G. P. Compo, 1998: A practical guide to wavelet analysis. *Bull. Amer. Meteor. Soc.*, **79**, 61–78.

Weng, H., and K. -M. Lau, 1994: Wavelets, period doubling, and time-frequency localization with application to organization of convection over the tropical western Pacific. *J. Atmos. Sci.*, **51**, 2523–2541.

Yanai, M., S. Esbensen, and J. H. Chu, 1973: Determination of bulk properties of tropical cloud clusters from large-scale heat and moisture budgets. *J. Atmos. Sci.*, **30**, 611–627.

Yang, S., and E. A. Smith, 1999: Moisture budget analysis of TOGA-COARE area using SSM/I retrieved latent heating and large scale Q_2 estimates. *J. Atmos. Oceanic Technol.*, **16**, 633–655.

Yang, S., and E. A. Smith, 2000: Vertical structure and transient behavior of convective-stratiform heating in TOGA-COARE from combined satellite-sounding analysis. *J. Appl. Meteor.*, **39**, 1491–1513.